Protection from Palmitate-Induced Mitochondrial DNA Damage Prevents from Mitochondrial Oxidative Stress, Mitochondrial Dysfunction, Apoptosis, and Impaired Insulin Signaling in Rat L6 Skeletal Muscle Cells

Larysa V. Yuzefovych, Viktoriya A. Solodushko, Glenn L. Wilson, and Lyudmila I. Rachek

Departments of Cell Biology and Neuroscience (L.V.Y., G.L.W., L.I.R.) and Physiology (V.A.S.), College of Medicine, University of South Alabama, Mobile, Alabama 36688

Saturated free fatty acids have been implicated in the increase of oxidative stress, mitochondrial dysfunction, apoptosis, and insulin resistance seen in type 2 diabetes. The purpose of this study was to determine whether palmitate-induced mitochondrial DNA (mtDNA) damage contributed to increased oxidative stress, mitochondrial dysfunction, apoptosis, impaired insulin signaling, and reduced glucose uptake in skeletal muscle cells. Adenoviral vectors were used to deliver the DNA repair enzyme human 8-oxoguanine DNA glycosylase/(apurinic/apyrimidinic) lyase (hOGG1) to mitochondria in L6 myotubes. After palmitate exposure, we evaluated mtDNA damage, mitochondrial function, production of mitochondrial reactive oxygen species, apoptosis, insulin signaling pathways, and glucose uptake. Protection of mtDNA from palmitate-induced damage by overexpression of hOGG1 targeted to mitochondria significantly diminished palmitate-induced mitochondrial superoxide production, restored the decline in ATP levels, reduced activation of c-Jun N-terminal kinase (JNK) kinase, prevented cells from entering apoptosis, increased insulin-stimulated phosphorylation of serine-threonine kinase (Akt) (Ser473) and tyrosine phosphorylation of insulin receptor substrate-1, and thereby enhanced glucose transporter 4 translocation to plasma membrane, and restored insulin signaling. Addition of a specific inhibitor of JNK mimicked the effect of mitochondrial overexpression of hOGG1 and partially restored insulin sensitivity, thus confirming the involvement of mtDNA damage and subsequent increase of oxidative stress and JNK activation in insulin signaling in L6 myotubes. Our results are the first to report that mtDNA damage is the proximal cause in palmitate-induced mitochondrial dysfunction and impaired insulin signaling and provide strong evidence that targeting DNA repair enzymes into mitochondria in skeletal muscles could be a potential therapeutic treatment for insulin resistance. (***Endocrinology*** **153: 92–100, 2012)**

Recently we have shown that the saturated free fatty acid (FFA) palmitate induced oxidative stress and caused significant mitochondrial DNA (mtDNA) damage, which correlated with concomitant mitochondrial dysfunction, apoptosis, and inhibition of insulin signaling in L6 myotubes (1). Therefore, we hypothesized that palmitate-induced mtDNA damage initiates processes that heighten oxidative stress causing a progressive mitochondrial and cellular dysfunction, which ultimately leads to apoptosis and impaired insulin signaling. Because mam-

ISSN Print 0013-7227 ISSN Online 1945-7170
Printed in U.S.A.

doi: 10.1210/en.2011-1442 Received June 30, 2011. Accepted October 27, 2011.
First Published Online November 29, 2011

Abbreviations: Ad, Adenovirus; Akt, serine-threonine kinase; 2DG, 2-deoxyglucose; FBS, fetal bovine serum; FFA, free fatty acid; GFP, green fluorescent protein; Glut4, glucose transporter 4; hOGG1, human 8-oxoguanine DNA glycosylase/(apurinic/apyrimidinic) lyase; IRS-1, insulin receptor substrate-1; JNK, c-Jun N-terminal kinase; MOI, multiplicity of infection; mtDNA, mitochondrial DNA; mtROS, mitochondrial ROS; MTS, mitochondrial targeting sequence; NEIL-1, endonuclease VIII-like 1; PM, plasma membrane; ROS, reactive oxygen species.

malian mtDNA encodes 13 polypeptides of the electron transport chain, two rRNA, and 22 tRNA, palmitate-induced damage to mtDNA causes an increase in the production of reactive oxygen species (ROS) by causing aberrant respiratory complex formation through the lack of coordination between components of the electron transport chains coded by mtDNA and those coded by nuclear DNA. The resultant production of ROS is able to initiate the formation of a vicious cycle, in which ROS cause damage to mtDNA, which causes further impairment in the formation of respiratory complexes and a concomitant increase in ROS production, which leads to even more damage to mtDNA. As the damage to mtDNA rises, there is a concomitant drop in ATP production resulting from the impairment of two electron reduction. The increased oxidative stress will exacerbate mitochondrial and cellular dysfunction, which ultimately leads to apoptosis and to activation of stress-activated kinases, which will compromise insulin signaling and thus lead to insulin resistance. To verify our hypothesis, we have used the approach of targeting the DNA repair enzyme human 8-oxoguanine DNA glycosylase/(apurinic/apyrimidinic) lyase (hOGG1) to mitochondria in L6 myotubes, which has been used previously by our group (2–4) and others (5, 6). Previously, it has been shown that targeting hOOG1 to mitochondria enhances mtDNA repair, decreases mitochondrial ROS (mtROS) production (5, 6) and protects different cell types from oxidant-mediated death (2–6). Here, we examined the effects of overexpression of hOGG1 targeted to mitochondria on mitochondrial dysfunction, mtROS production, oxidative-stress mediated signal transduction, and insulin signaling pathways in skeletal muscle L6 myotubes, exposed to palmitate. L6 myotubes were transduced with an adenoviral vector, containing the gene for hOGG1 downstream of the mitochondrial targeting sequence (MTS) from manganese superoxide dismutase and the gene for green fluorescent protein (GFP) to monitor the efficiency of transduction. Adenoviral vector without the MTS-hOGG1 insert, but containing GFP, was used as a negative control. We found that protection of mtDNA from palmitate-induced damage by mitochondrial overexpression of hOGG1 also protects mitochondrial function in L6 myotubes after palmitate treatment. Also, palmitate-induced mitochondrial-derived oxidative stress, activation/phosphorylation of oxidative stress-activated c-Jun N-terminal kinase (JNK) kinase, and apoptosis were reduced in the MTS-OGG1-transduced cells compared with the control cultures. Most importantly, we have shown that attenuation of palmitate-induced mtDNA damage leads to increased insulin sensitivity, which had been compromised by palmitate in L6 myotubes.

Our study is the first to show that mtDNA damage is critical and primary to the development of mitochondrial dysfunction and consequent oxidative stress and thus decreased insulin sensitivity in L6 myotubes. Previously, it has been demonstrated that depletion of mtDNA caused impaired glucose utilization in L6 skeletal muscle cells, suggesting a crucial role for mtDNA in the decrease of insulin sensitivity and glucose uptake in skeletal muscle cells (7). Additionally, that mtDNA is a prime target for ROS damage is illustrated by the fact that increased mtDNA damage and deletions have been observed in mice with symptoms resembling metabolic syndrome (8). This mouse model was created by knocking out the gene encoding the DNA repair enzyme NEIL1 (endonuclease VIII-like 1) (9). Recently, mitochondrial localization of NEIL1 has been reported, thus linking NEIL1 to repair of oxidative damage in mtDNA (10). In agreement with this notion of a destructive role for ROS on mtDNA in type 2 diabetes is the finding that there are increased mtDNA mutations in skeletal muscle from type 2 diabetes patients (11). Also, a very recent study showed that insulin sensitivity in skeletal muscle is decreased in adult subjects with m.3243A>G mutation in mtDNA (12).

Additionally, we have shown that SP-600125, a specific inhibitor of JNK, mimicked the effect of mitochondrial overexpression of hOGG1 and significantly increased palmitate-inhibited glucose uptake. This finding demonstrated the involvement of mtDNA damage in the subsequent increase of oxidative stress and JNK activation leading to subsequent impaired insulin signaling and reduced insulin-stimulated glucose uptake in L6 myotubes. Overall, these results demonstrate that palmitate-induced mtDNA damage, mitochondrial dysfunction, apoptosis, and impaired glucose utilization can be prevented by targeting of hOGG1 to mitochondria, thus confirming that mtDNA damage triggers both palmitate-induced mitochondrial dysfunction and the development of impaired insulin sensitivity in L6 myotubes.

Materials and Methods

Materials

DMEM was from Invitrogen, Inc. (Carlsbad, CA), fetal bovine serum (FBS) was from HyClone (Logan, UT). Palmitate, SP-600125, BSA (fatty acid free), insulin (from bovine pancreas), and penicillin/streptomycin were from Sigma (St. Louis, MO). 2-Deoxy-D-[^{3}H] glucose was purchased from PerkinElmer (Shelton, CO).

Cell culture and treatment

Rat L6 skeletal muscle cells were obtained from American Type Culture Collection (Manassas, VA). Cells were grown in

DMEM supplemented with 10% FBS and 50 μg/ml penicillin/streptomycin in 5% CO_2 at 37 C. For these studies, L6 myoblasts were plated in culture dishes, six- or 24-well plates at 1–2 $\times$ 10^5 cells/ml, and used at the myotube stage of differentiation as described previously (1, 13) Differentiation was achieved by culturing preconfluent cells in the "differentiation" DMEM (1 g/liter glucose, 2% FBS instead of 10% in the "growth" media) for 5–7 d. The differentiation media was changed every other day. Reduction of serum allowed cell-to-cell fusion and formation of myotubes. A stock concentration of palmitate was prepared as discussed previously (1, 13). Control cells were treated with drug diluent only [2% BSA in the serum-free DMEM (1 g/liter glucose)]. In some experiments, cells were preincubated with 25 μM SP-600125 for 30 min before palmitate treatment. A stock concentration of SP-600125 was dissolved in dimethylsulfoxide. Control cultures, not treated with SP-600125, received the same concentration of dimethylsulfoxide as in the compound-treated cultures. In the serine-threonine kinase (Akt) (Ser473) and insulin receptor substrate-1 (IRS-1) tyrosine phosphorylation, and for glucose transporter 4 (Glut4) translocation experiments, L6 myotubes were incubated with palmitate for 16 h, followed by incubation in the absence or presence of insulin (100 nM) during the last 15 min of treatment.

Adenovirus transduction

Adenoviruses containing MTS-hOGG1 and GFP were kindly provided by Mark Kelley (Indiana University, Indianapolis, IN) and have been described previously (6). Adenoviruses were amplified using the human embryogenic kidney cell line (HEK-293). Lysates obtained were titrated using Adeno-X Rapid Titer kit (CLONTECH Laboratories, Inc., Mountain View, CA). Initial experiments were done to find the most efficient multiplicity of infection (MOI). We found that an MOI of 70 gave us 100% GFP positive cells and the greatest amount of hOGG1 in mitochondria [for adenovirus (Ad)-MTS-hOGG1]. In addition, we have evaluated cell viability at MOI of 70 for both Ad-MTS-hOGG1and Ad-GFP-transduced cells using trypan blue exclusion method as previously described (13). Compared with control untreated cells, adenovirus transduction did not affect cells viability, which was 98.5 $\pm$ 1.2 and 99 $\pm$ 1.4 for Ad-GFP and Ad-MTS-hOGG1, respectively. For all further experiments, adenoviral vectors were added to cells in the differentiated media at an MOI of 70. After 48 h of transduction, those cells were exposed to palmitate for the indicated time.

Assay for mtDNA damage

L6 myotubes were transduced with adenoviruses as described above and then exposed to palmitate for 6 h. DNA isolation and quantitative Southern blottings were performed as previously described (1, 4, 13) with some modifications. Cells were lysed in 10 mM Tris-HCI (pH 8.0), 1 mM EDTA (pH 8.0), 0.5% sodium dodecyl sulfate, and 0.3 mg/ml proteinase K overnight at 37 C. High molecular weight DNA was extracted with phenol, treated with ribonuclease (to a final concentration of 1 μg/ml), and digested to completion with *Bam*HI (10 U/μg of DNA overnight). Digested samples were precipitated, resuspended in Tris-EDTA buffer, and precisely quantified using a Hoefer TKO 100 minifluorometer and TKO standard kit. Samples containing 5 μg of DNA were heated at 70 C for 15 min and then cooled at room temperature for 20 min. A sodium hydroxide solution then was added to a final concentration of 0.1 N, and samples were incubated for 15 min at 37 C. This alkali treatment produced single strand breaks at all abasic or sugar-modified sites in the DNA. Gel electrophoresis and vacuum transfer were carried out as described previously (1, 4, 13). After prehybridization, membranes were hybridized with a denatured PCR-generated mitochondrial probe (1, 4, 13), washed according to the manufacturer's suggestions, and autoradiographed. The mitochondrial probe used to hybridize mtDNA was a 745-bp PCR product that is a part of the cytochrome c oxidase 1 gene. This 745-bp PCR product recognized a 10.8-kb restriction fragment when hybridized to rat DNA digested with *Bam*HI (1, 4, 13). The resultant band images were scanned and analyzed using Fujifilm Image Gauge version 2.2 (FujiFilm USA, Stamford, CT) software. Break frequency was determined using the Poisson expression ($s = -\ln P_o$, where s is the number of breaks per fragment and P_o is the fraction of fragments free of breaks) as previously described (1, 4, 13). Break frequency for nuclear DNA fragments was calculated by scanning similar size fragments ($\sim$11 kb) from the ethidium bromide-stained gel photographs as discussed previously (13).

Measurement of ATP levels

Cells were grown in 24-well culture plates, differentiated, and transduced with adenoviruses. Forty-eight hours after transduction, cells were treated with 0.5 or 1 mM palmitate for 24 h. To determine the total cellular ATP level, an ATP bioluminescence assay kit (Roche, Mannheim, Germany) was used as previously described (1, 13, 14).

Cell viability

The CellTiter 96 assay (Promega, Madison, WI), a colorimetric method for determining the number of viable cells by assessing mitochondrial function, was performed 24 h after exposure to 0.5 or 1 mM palmitate, as previously described (1, 13, 14). The reagent was added to culture wells, and the cells were incubated for 2 h. OD was read at 490 nm in a microplate reader. Data are displayed as a percentage of untreated controls.

Mitochondrial ROS production

Transduced L6 myotubes were exposed to the indicated concentrations of palmitate for 24 h and then analyzed for mtROS production. MitoSOX Red, a mitochondrial superoxide indicator for live cell imaging (Invitrogen, Inc.), was employed to analyze mitochondrial superoxide generation within L6 myotube mitochondria as described (1). Values are shown as a percentage of the corresponding untreated control.

Subcellular fractionation, protein isolation, immunoprecipitation, and Western blot analysis

Plasma membrane (PM) preparations were performed according to the method of Mitsumoto and Klip (15). Mitochondrial, nuclear, and cytosolic protein fractions were isolated from one 60-mm dish of each cell type (MTS-hOGG1-transduced and GFP only-transduced cells) by differential centrifugation as described previously (2–4). Protein extracts for total cellular fractions were isolated in Cell Lysis Buffer (Cell Signaling, Beverly, MA) supplemented with 0.1 mg phenylmethylsulfonylfluoride and a 1/100 dilution of the protease and phosphatase inhibitor cocktails (Sigma). The cells were scraped to dislodge them from the bottom of the dishes and then passed four times through a

1cc-gauge syringe (Becton Dickinson, Franklin Lakes, NJ). Samples were centrifuged for 10 min at 14,000 × *g*, and the supernatants were used for Western blottings. Protein concentrations were determined using the Bio-Rad protein dye microassay (Bio-Rad, Hercules, CA). For immunoprecipitation of IRS-1, 200 μg of total cell lysates were used, and samples were resolved using 8% SDS-PAGE gels. SDS-PAGE and transfer of separated proteins to nylon or polyvinylidene fluoride-membranes were performed as previously described (1, 4, 13). The antibodies used were to hOGG1 (Novus Biologicals, Littleton, CO); cytochrome c (PharMingen, San Diego, CA); actin (Sigma); caspase-3, phospho-Akt (Ser473), total-Akt, phospho-stress-activated protein kinase/JNK (T183/Y185), and total stress-activated protein kinase/JNK (Cell Signaling); IRS-1 (Millipore, Temecula, CA); and lamin A and pTyr (Santa Cruz Biotechnology, Inc., Santa Cruz, CA). Complexes formed were detected with horseradish peroxidase-conjugated antimouse IgG or antirabbit IgG antibodies (Promega) using chemiluminescent reagents (Cell Signaling). Where indicated, the resultant band images were scanned and analyzed using Fujifilm Image Gauge version 2.2 software.

2-Deoxy-D-[^{3}H] glucose uptake

L6 myotubes were cultured in six-well plates, transduced with adenoviruses, and treated with medium containing palmitate or BSA as a control, as indicated, and 2-deoxyglucose (2DG) uptake was performed as previously described (16). Nonspecific uptake was measured in the presence of 10 μM cytochalasin B and was subtracted from all values. Radioactivity was measured by liquid scintillation counting. Protein concentration was measured using a Bradford assay.

Statistical analysis

Data are expressed as means ± SE. Differences between two groups were assessed using unpaired, two-tailed Student's *t* test. Data involving more than two groups were performed using one-way ANOVA (Prism; GraphPad, San Diego, CA) followed by Bonferroni analysis where appropriate. Statistical significance was determined at the 0.05 level.

Results

Human OGG1 expression in mitochondria of L6 myotubes

First, we performed experiments to determine the most efficient MOI of MTS-hOGG1 and GFP-expressing adenoviruses for transduction. Mitochondrial extracts were prepared from MTS-hOGG1- and GFP-transduced cultures incubated with various MOI of adenoviruses. Mitochondria were isolated by differential centrifugation, and Western blottings were performed using a polyclonal antibody to hOGG1 (Fig. 1A). Even loading was confirmed by Ponceau staining of the membrane after transfer. As shown in Fig. 1A, the greatest amount of hOGG1 in mitochondria was observed at an MOI of 70 of MTS-hOGG1, whereas the mitochondrial hOGG1 was undetectable at the same MOI of the control adenovirus expressing only GFP. Also, to prove that hOOG1 is targeted exclusively to mitochondria and evaluate possible leakage expression in nucleus and cytoplasm, we isolated nuclear and cytosolic fractions from GFP- or MTS-hOGG1-transduced cultures and performed Western blotting using human OGG1 antibody. As shown in Fig. 2B, no difference was observed in protein bands (which represent endogenous OGG1) in lanes containing nucleus- or cytosolic-enriched fractions, thus confirming that MTS-hOGG1 is predominantly expressed in mitochondria without leakage expression in other cell compartments.

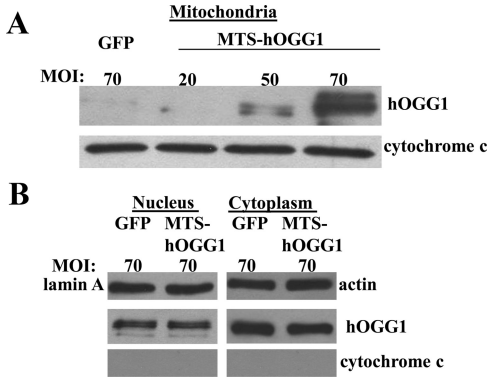

FIG. 1. Targeting of hOGG1 to mitochondria from L6 myotubes. A, Adenoviral vectors (GFP or MTS-hOGG1) were added to cells in differentiation media at the indicated MOI. After a 48-h transduction, mitochondrial fractions were isolated from the transduced L6 myotubes, and Western blot analysis was performed using hOGG1 antiserum. Immunodetection of cytochrome c was performed to assure mitochondrial localization. B, Nuclear and cytosolic fractions were isolated from L6 myotubes transduced with GFP or MTS-hOGG1 viruses at a MOI of 70. Equal loading was confirmed using Ponceau staining of the membrane. Lamin A and actin were used to indicate nuclear and cytosolic localization, respectively. To exclude possible contamination from mitochondrial fractions, a separate portion of the same blot was probed with cytochrome c.

Targeting of hOGG1 to mitochondria prevented palmitate-induced mtDNA damage and mitochondrial dysfunction in L6 myotubes

To evaluate mtDNA damage, MTS-hOGG1- and GFP-transduced L6 myotubes were exposed to 0.5 or 1 mM palmitate conjugated to 2% BSA for 6 h. Control cells were incubated with diluent (2% BSA) only. Cells were lysed, total DNA was isolated, and quantitative Southern hybridizations were performed using a mtDNA-specific probe. Also, to rule out the possible beneficial effect of hOGG1 overexpression not related to mtDNA protection but to nuclear DNA protection, the damage to nuclear DNA was assessed in both MTS-hOGG1- and GFP-transduced L6 by performing a densitometric scan of the DNA in the ethidime bromide stained alkaline agarose gel used for the Southern blotting. The results demonstrated a significant decrease only in palmitate-induced mtDNA damage in MTS-hOGG1-transduced L6 myotubes compared

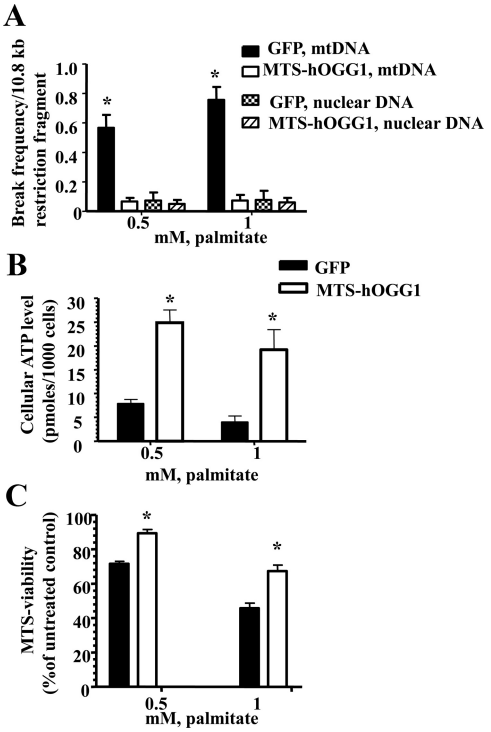

FIG. 2. Overexpression of hOGG1 in mitochondria from L6 myotubes prevents palmitate-induced mtDNA damage and increased mitochondrial function. A, Break frequency per 10.8-kb fragment of nuclear and mtDNA after 6 h of treatment with the indicated concentrations of palmitate ($n \geq 3$). *, $P < 0.05$ *vs.* all other groups. B, ATP levels were increased in L6 myotubes transduced with MTS-hOGG1 adenoviruses after palmitate treatment. Cells were transduced with the adenoviruses for 48 h and then treated with the indicated concentration of palmitate, and ATP production was measured. The mean results ± SE are shown ($n \geq 3$). *, $P < 0.05$ *vs.* GFP-transduced cells treated with the same concentration of palmitate. C, Mitochondrial function is increased in MTS-hOGG1-expressing myotubes 24 h after exposure to indicated concentrations of palmitate. The average results ± SE are shown ($n = 3$). *, $P < 0.05$ *vs.* GFP-transduced cells treated with the same concentration of palmitate.

with cells transduced with only GFP, whereas there was no difference in nuclear DNA damage between MTS-hOGG1- and GPP-transduced myotubes after treatment with palmitate (Fig. 2A). Additionally, for measuring ATP level, MTS-hOGG1- or GFP-transduced L6 myotubes were grown in 24-well culture plates, treated with palmitate for 24 h, washed twice with PBS, and ATP production was measured. Control cultures were exposed to diluent only for the same amount of time. As can be seen in Fig. 2B, ATP levels were significantly higher in MTS-hOGG1-transduced cells as compare with GFP-transduced cells after incubation with the same concentrations of palmitate. Also, mitochondrial function was evaluated in MTS-hOGG1 or GFP-transduced cultures treated with 0.5 or 1 mM palmitate for 24 h. As shown in Fig. 2C, MTS-hOGG1-transduced myotubes showed significantly greater viability compared with control GFP-transduced L6 cells.

Effect of hOGG1 expression in mitochondria on mtROS production, JNK activation, and apoptosis in L6 myotubes

Next, we evaluated whether protection from palmitate-induced mtDNA damage would have an effect on mtROS generation in L6 myotubes after palmitate treatment. MTS-hOGG1- or GFP-transduced L6 myotubes were grown in 24-well culture plates, treated with palmitate (0.5 or 1 mM) for 24 h, and mtROS generation was measured as described in *Materials and Methods*. As shown in Fig. 3A, palmitate treatment significantly increased mitochondrial superoxide generation in GFP-transduced myotubes, with only a slight increase in mtROS generation in MTS-OGG1-transduced L6 myotubes. Because activation of stress-activated protein kinase JNK has been implicated in both the modulation of apoptosis (17) and impaired insulin sensitivity (18, 19), we compared the phosporylation/activation level of JNK in MTS-hOGG1

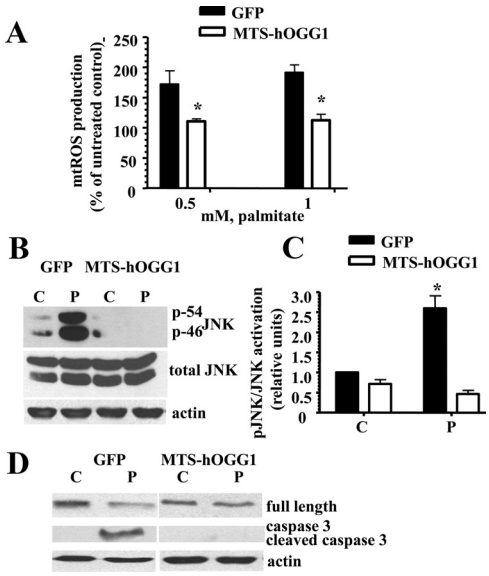

FIG. 3. Targeting of hOGG1 to mitochondria in L6 myotubes protected against palmitate-induced mtROS generation, reduced activation of JNK kinase, and prevented cells from undergoing apoptosis. A, Mitochondrial superoxide production in MTS-hOGG1- and GFP-transduced L6 myotubes treated with the indicated concentrations of palmitate for 24 h. Cells were analyzed in a fluorescent plate reader, and the increase in ROS production was calculated as a percentage increase compared with control. The mean results ± SE are shown ($n \geq 3$). *, $P < 0.05$ *vs.* GFP-transduced cells treated with the same concentration of palmitate. B, Adenovirus-transduced L6 myotubes were exposed to control medium (C) (2% BSA) or medium containing 1 mM palmitate (P). Total cell lysates were isolated and analyzed by Western blotting with the indicated antibodies. Equal loading was confirmed using antiactin antibody. C, The values from densitometry from three (pJNK) independent experiments were normalized to the level of total JNK and expressed as fold of difference normalized to GFP control data ± SE; *, $P < 0.05$ *vs.* all other groups. D, Results of the Western blottings using caspase-3 antibodies which recognize the full-length (35-kD) and the large (17 kD) fragment of caspase-3 resulting from its cleavage. Equal loading was confirmed by loading antiactin antibody.

or GFP-transduced L6 myotubes after incubation with palmitate. As shown in Fig. 3, B and C, targeting of hOGG1 to mitochondria inhibited palmitate-induced JNK phosphorylation. Previously, we have shown that palmitate induced apoptosis in L6 myotubes (1, 13). To determine whether the protective effect of hOGG1 on mtDNA integrity was correlated with inhibition of palmitate-induced apoptosis, we used Western blot analysis of caspase-3 activation (Fig. 3D). Twenty-four hours after palmitate treatment, activated caspase-3 was found in GFP-L6 myotubes (Fig. 3D), whereas cleavage of caspase-3 was significantly decreased in MTS-hOGG1 cultures compared with the GFP-containing cultures.

Mitochondrial targeting of hOGG1 prevented palmitate-induced inhibition of insulin signaling and thus increased insulin-stimulated GLUT4 translocation to the PM

To access whether mtDNA damage is implicated in palmitate-induced inhibition of insulin signaling, we performed the experiments described below. First, we evaluated the acute, insulin-mediated tyrosine phosphorylation of IRS-1 (Fig. 4, A and C) and showed that mitochondrial targeting of hOGG1 restored insulin-dependent phosphorylation of IRS-1 in L6 myotubes, which was decreased by palmitate. Interestingly, palmitate treatment decreased total levels of IRS1, whereas mitochondrial overexpression of hOGG1 also restored total protein levels of IRS-1 (Fig. 4, A and B). Second, we compared phosphorylated Akt levels in total protein fractions isolated from MTS-hOGG1- or GFP-transduced L6 myotubes treated with palmitate. As shown in Fig. 4, D and E, mitochondria-targeted hOOG1 prevented palmitate-induced inhibition of insulin-stimulated phosphorylation of Akt (Ser473). We next examined the effect of mitochondrial overexpression of hOGG1 on the translocation of GLUT4 to the PM and showed increased insulin-dependent GLUT4 translocation to the PM in the fractions isolated from MTS-hOGG1-transduced L6 cells treated with palmitate (Fig. 4, G and F).

Human OGG1 targeting to mitochondria protects from palmitate-induced decrease in insulin-stimulated glucose uptake in L6 myotubes

To show that mtDNA damage contributed to palmitate-induced decrease in insulin-stimulated glucose uptake in L6 myotubes, we measured 2DG uptake in L6 myotubes transduced with MTS-hOGG1 or GFP adenoviruses. Insulin stimulation similarly increased 2DG uptake in both GFP- and MTS-hOGG1-transduced cultures treated with 2% BSA (control cultures, see Fig. 5A). Interestingly, we found that palmitate also increased basal 2DG glucose uptake equally (~1.7-fold) in both GFP- and MTS-OGG1-transduced cultures, which is in agreement with the recent findings obtained by other groups (20, 21). At the same time, MTS-hOGG1-transduced cells showed greater insulin-stimulated 2DG compared with GFP cul-

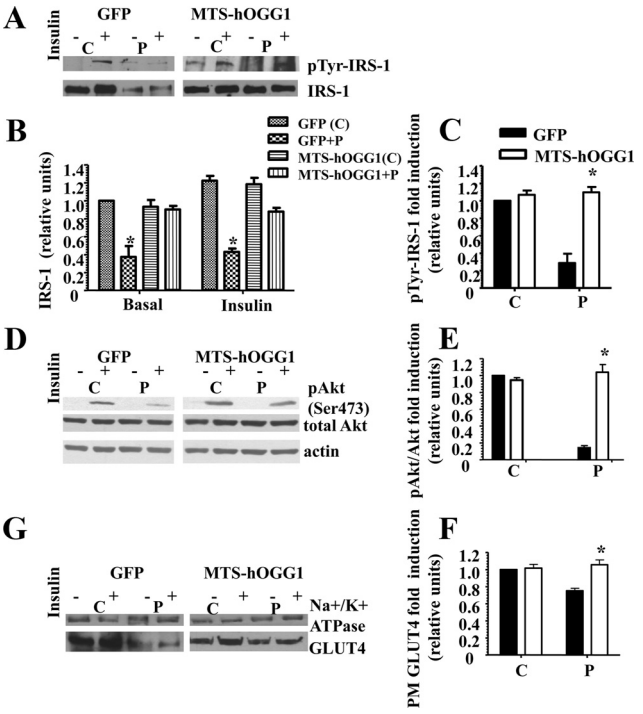

FIG. 4. Targeting of hOGG1 to mitochondria in L6 myotubes ameliorated palmitate-mediated inhibition of insulin-induced. A, C tyrosine phosphorylation of IRS-1. D and E, Akt (Ser473) phosphorylation. G and F, GLUT4 translocation to the PM. MTS-hOGG1- or GFP-transduced L6 myotubes were exposed to control medium (C) (2% BSA) or to medium containing 1 mM palmitate (P) for 16 h and then treated with insulin as described in *Materials and Methods*. Total cell lysates or PM (as specified) were isolated and analyzed by Western blot analysis with the indicated antibodies. A, *top panel*, IRS-1 was immunoprecipitated from 200 μg of total cell lysates, and Western blottings were performed using an pTyr antibody. *Bottom*, Representative Western blotting of total IRS-1. B, Densitometry data for the total IRS-1 protein levels normalized to GFP control data ($n \geq 3$). *, $P < 0.05$ *vs.* all other groups. C, Densitometry data for insulin dependent (pTyr-IRS-1) were normalized to GFP (control plus insulin) data and presented as means ± SE ($n \geq 3$). *, $P < 0.05$ *vs.* GFP-transduced cells treated with palmitate. D, Representative blots from at least three independent experiments for phosphorylation of Akt (Ser473) are shown. Total cell lysates were used. E, The values from densitometry from at least three (pAkt) independent experiments were normalized to the level of total Akt and expressed as fold of difference after addition of insulin normalized to the GFP (control plus insulin) data. The mean results ± SE are shown. *, $P < 0.05$ *vs.* GFP-transduced cells treated with palmitate. G, PM were isolated from adenovirus-transduced L6 myotubes, as described in *Materials and Methods*, and proteins were analyzed by Western blotting using GLUT4 antibody. Immunodetection of the α-subunit of Na+/K+-ATPase was performed to confirm PM localization. The values from densitometry performed on three to four independent GLUT4 translocation to PM independent experiments were normalized to the level of α-subunit of Na+/K+-ATPase and then normalized to the GFP (control plus insulin) data ± SE ($n \geq 3$). *, $P < 0.05$ *vs.* GFP-transduced cells treated with palmitate.

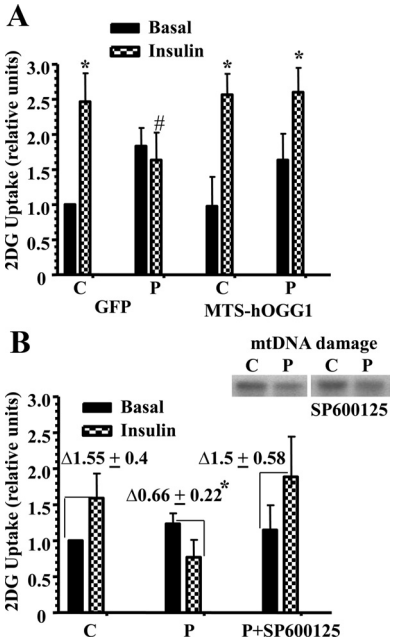

FIG. 5. Targeting of hOGG1 to mitochondria in L6 myotubes protected against palmitate-induced decrease in insulin-stimulated 2DG uptake. A, MTS-hOGG1- and GFP-transduced L6 myotubes were treated with 2% BSA (C, 2% BSA) or 2% BSA plus 1 mM palmitate (P) for 16 h. After that, cells were incubated in the absence or presence of insulin for 20 min and then for 5 min with 2DG, and uptake was measured as described in *Materials and Methods*. Values were normalized to the GFP control basal data and are the means ± SE ($n \geq 3$). *, $P < 0.05$ *vs.* respective basal; #, $P < 0.05$ *vs.* all other groups treated with insulin. B, *graph*, Effect of a JNK inhibitor on palmitate-induced inhibition of insulin-stimulated 2DG uptake. L6 myotubes were incubated in the medium containing only 2% BSA (C, Control) (2% BSA) or 2% BSA plus 1 mM palmitate (P) in the presence or absence of the JNK inhibitor, SP-600125 for 16 h before stimulation with insulin and measurement of 2DG uptake. Values were normalized to the control basal data and are the means ± SE ($n \geq 3$). Δ, Fold induction on insulin. *, $P < 0.05$ *vs.* both control and palmitate plus SP-600125. B, *panel above graph*, Effect of JNK inhibitor on palmitate-induced mtDNA damage. L6 myotubes were incubated with 2% BSA (C) or 2% BSA plus 1 mM palmitate (P) in the presence or absence of the JNK inhibitor, SP-600125 for 6 h. mtDNA damage was evaluated as described in *Materials and Methods*.

tures after treatment with 1 mM palmitate (Fig. 5A), thus proving that mitochondrial targeting of hOGG1 made cells more insulin sensitive after palmitate treatment. Previously, we have shown that SP-600125, a specific inhibitor of JNK, improved insulin-stimulated Akt (Ser473) phosphorylation and prevented caspase-3 activation in L6 myotubes exposed to palmitate (1). In the present study, we examined the involvement of JNK in palmitate-induced decrease in glucose uptake and performed 2DG uptake studies using a specific inhibitor of JNK, SP-600125. As shown in Fig. 5B, *graph*, SP-600125 significantly improved palmitate-induced inhibition of insulin-stimulated 2DG uptake, thus confirming the involvement of JNK into palmitate-induced impaired insulin sensitivity in L6 myotubes. To confirm that JNK activation is really downstream of palmitate-induced mtDNA damage and thus to rule out previously discussed (22) possibility that JNK signaling is required for DNA repair, we have evaluated the effect of JNK inhibitor on palmitate-induced mtDNA damage. As shown in Fig. 5B, *top panel*, SP-600125 did not affect palmitate-induced mtDNA damage, therefore confirming that JNK activation is in fact downstream of palmitate-induced mtDNA damage.

Discussion

This study reveals a novel mechanism that links palmitate-induced mtDNA damage to mitochondrial dysfunction and thus to inhibition of insulin signaling pathways and consequent decrease in insulin-stimulated glucose uptake in L6 myotubes. Based on recent publications demonstrating that oxidative stress resulting from ROS-induced mitochondrial dysfunction contributes to insulin resistance (23–26) and our previous studies that palmitate induced mtDNA damage, mtROS, and mitochondrial dysfunction (1), we hypothesized that palmitate-induced damage to mtDNA could further exacerbate the oxidative stress in mitochondria and thereby heighten the production of mitochondrial-derived ROS. The results of this study show that targeting this DNA repair enzyme to mitochondria prevented palmitate-induced 1) mtDNA damage, 2) mtROS production, 3) mitochondrial dysfunction, 4) JNK activation and inhibition of apoptosis and insulin signaling pathways, and 5) decrease in insulin-stimulated glucose uptake. The major principal and novel finding of this study is that mtDNA damage is a contributor and a proximal cause of palmitate-induced impaired insulin sensitivity in L6 myotubes. Although a few groups have assessed the biological impact of modulating mtROS levels on insulin signaling (23–26), we are in unique position because our study is the first that explains the origin of mtROS and identifies mtDNA as both a target and key source of mitochondrial derived ROS. To the best of our knowledge, no studies have been performed to determine the link between mtDNA damage, mitochondrial dysfunction, mtROS, and ROS-driven signaling leading to the insulin resistance.

A study by Houstis *et al.* (27) confirmed that insulin resistance can be prevented by blocking the increase in ROS levels, including mtROS. Additionally, a more recent study showed that mitochondrial superoxide production is a unifying element of insulin resistance (26). Also, a very recent study by the Shulman group showed that targeted expression of catalase to mitochondria prevented age-associated reductions in mitochondrial function and insulin resistance (25). Elevated saturated FFA levels have numerous deleterious effects on mitochondria, including increased production of ROS (1, 13, 19, 24, 26, 28). More-

over, it has been postulated that impaired mitochondrial function could directly contribute to insulin resistance by impairing the production of ATP, which is essential for the support of all the reactions in the insulin signaling pathway that require phosphorylation (29). It is still arguable whether mitochondrial dysfunction precedes or results from insulin resistance in the skeletal muscle of type 2 diabetes patients, or whether these are parallel processes. A recent study by Bonnard *et al*. (23) showed that mitochondrial dysfunction results from oxidative stress in the skeletal muscle of diet-induced insulin-resistant mice (23). Also, data obtained in this study and in the more recent work describing the prevention of age-associated insulin resistance in mice with targeted overexpression of human catalase in mitochondria (25) suggested that mitochondrial dysfunction *per se* is not the initial event that triggers the inhibition of insulin action, as observed in type 2 diabetes, but it is rather the increased oxidative stress that promotes mitochondrial alterations, lipid accumulation, and insulin resistance.

Previous studies have shown that multiple stress-sensitive kinases are activated by oxidative stress, which leads to the pathological condition of insulin resistance (9, 30), and protective strategies, which include using ROS scavengers and antioxidants have improved insulin signaling both *in vitro* and *in vivo* (31, 32). One such major kinase target for oxidative stress is JNK, activation of which by oxidative stress has been previously shown to interfere with insulin action both *in vivo* (fat-fed animals) and in L6 myotubes treated with hydrogen peroxide by decreasing insulin-stimulated tyrosine phosphorylation of IRS-1 (31). Furthermore, antioxidants preserved redox balance, inhibited JNK activation, and thus improved insulin signaling in both fat-fed animals and in L6 myotubes treated with hydrogen peroxide (31). Also, α-lipoic acid has been shown to improve insulin sensitivity in skeletal muscle both *in vivo* and *vitro* through inhibition of JNK activation (32). Additionally, it has been found that selective inhibition of JNK kinase in adipose tissue protected against diet-induced obesity and improved insulin sensitivity in both liver and skeletal muscle in mice (33). Previously (1), and in this study, we have shown that palmitate induced JNK activation in L6 myotubes. Our current results demonstrate that targeting of hOGG1 to mitochondria decreased mtROS and thus prevented activation of JNK, leading to improvement of palmitate-mediated inhibition of insulin-induced: 1) tyrosine phosphorylation of IRS-1; and 2) Akt (Ser473) phosphorylation, and thus to overall increased insulin-stimulated translocation of GLUT4 to the PM and the consequent restoration of insulin-stimulated glucose uptake in L6 myotubes, which had been inhibited by palmitate. Also, as we have shown previously (1), addition of a specific JNK inhibitor, SP-600125, protected against both palmitate-induced inhibition of insulin-stimulated Akt (Ser473) phosphorylation and apoptosis in L6 myotubes. Moreover, in the current study, we have shown that SP-600125 also increased palmitate-inhibited insulin-stimulated glucose uptake, thus mimicking the effect of hOGG1 overexpression in mitochondria in L6 myotubes.

Based on our data, we believe that we have confirmed our hypothesis and have proven that palmitate-induced mtDNA damage, through increase of mtROS generation and consequent JNK activation, triggers palmitate-induced apoptosis and decrease in insulin-stimulated glucose uptake in skeletal muscle cells. Taken together, our findings demonstrate that protection from mtDNA damage by modulating the level of mitochondrial OGG1 may provide a new therapeutic strategy for treating insulin resistance in skeletal muscles.

Acknowledgements

We thank Dr. Mark Kelley (Indiana University, Indianapolis, IN) for providing stock of adenoviruses, Dr. Ryan Vyatt for providing technical expertise on glucose uptake experiments, and Luanne Galanopoulos for help in preparation the manuscript.

Address all correspondence and requests for reprints to: Lyudmila I. Rachek, Department of Cell Biology and Neuroscience, University of South Alabama, Mobile, Alabama 36688. E-mail: lrachek@jaguar1.usouthal.edu.

This work was supported by the National Institutes of Health Grant DK073808 (to L.I.R.).

Disclosure Summary: The authors have nothing to disclose.

References

1. **Yuzefovych L, Wilson G, Rachek L** 2010 Different effects of oleate vs. palmitate on mitochondrial function, apoptosis, and insulin signaling in L6 skeletal muscle cells: role of oxidative stress. Am J Physiol Endocrinol Metab 299:E1096–E1105
2. **Rachek LI, Grishko VI, Musiyenko SI, Kelley MR, LeDoux SP, Wilson GL** 2002 Conditional targeting of the DNA repair enzyme hOGG1 into mitochondria. J Biol Chem 277:44932–44937
3. **Rachek LI, Grishko VI, Ledoux SP, Wilson GL** 2006 Role of nitric oxide-induced mtDNA damage in mitochondrial dysfunction and apoptosis. Free Radic Biol Med 40:754–762
4. **Rachek LI, Thornley NP, Grishko VI, LeDoux SP, Wilson GL** 2006 Protection of INS-1 cells from free fatty acid-induced apoptosis by targeting hOGG1 to mitochondria. Diabetes 55:1022–1028
5. **Ricci C, Pastukh V, Leonard J, Turrens J, Wilson G, Schaffer D, Schaffer SW** 2008 Mitochondrial DNA damage triggers mitochondrial-superoxide generation and apoptosis. Am J Physiol Cell Physiol 294:C413–C422
6. **Kim J, Xu M, Xo R, Mates A, Wilson GL, Pearsall 4th AW, Grishko V** 2010 Mitochondrial DNA damage is involved in apoptosis caused

by pro-inflammatory cytokines in human OA chondrocytes. Osteoarthritis Cartilage 18:424–432
7. **Park SY, Choi GH, Choi HI, Ryu J, Jung CY, Lee W** 2005 Depletion of mitochondrial DNA causes impaired glucose utilization and insulin resistance in L6 GLUT4myc myocytes. J Biol Chem 280:9855–9864
8. **Vartanian V, Lowell B, Minko IG, Wood TG, Ceci JD, George S, Ballinger SW, Corless CL, McCullough AK, Lloyd RS** 2006 The metabolic syndrome resulting from a knockout of the NEIL1 DNA glycosylase. Proc Natl Acad Sci USA 103:1864–1869
9. **Qiao LY, Goldberg JL, Russell JC, Sun XJ** 1999 Identification of enhanced serine kinase activity in insulin resistance. J Biol Chem 274:10625–10632
10. **Hu J, de Souza-Pinto NC, Haraguchi K, Hogue BA, Jaruga P, Greenberg MM, Dizdaroglu M, Bohr VA** 2005 Repair of formamidopyrimidines in DNA involves different glycosylases: role of the OGG1, NTH1, and NEIL1 enzymes. J Biol Chem 280:40544–40551
11. **Liang P, Hughes V, Fukagawa NK** 1997 Increased prevalence of mitochondrial DNA deletions in skeletal muscle of older individuals with impaired glucose tolerance: possible marker of glycemic stress. Diabetes 46:920–923
12. **Lindroos MM, Majamaa K, Tura A, Mari A, Kalliokoski KK, Taittonen MT, Iozzo P, Nuutila P** 2009 m. 3243A>G mutation in mitochondrial DNA leads to decreased insulin sensitivity in skeletal muscle and to progressive β-cell dysfunction. Diabetes 58:543–549
13. **Rachek LI, Musiyenko SI, LeDoux SP, Wilson GL** 2007 Palmitate induced mitochondrial deoxyribonucleic acid damage and apoptosis in l6 rat skeletal muscle cells. Endocrinology 148:293–299
14. **Rachek LI, Yuzefovych LV, Ledoux SP, Julie NL, Wilson GL** 2009 Troglitazone, but not rosiglitazone, damages mitochondrial DNA and induces mitochondrial dysfunction and cell death in human hepatocytes. Toxicol Appl Pharmacol 240:348–354
15. **Mitsumoto Y, Klip A** 1992 Development regulation of the subcellular distribution and glycosylation of GLUT1 and GLUT4 glucose transporters during myogenesis of L6 muscle cells. J Biol Chem 267:4957–4962
16. **Huang C, Somwar R, Patel N, Niu W, Török D, Klip A** 2002 Sustained exposure of L6 myotubes to high glucose and insulin decreases insulin-stimulated GLUT4 translocation but upregulates GLUT4 activity. Diabetes 51:2090–2098
17. **Tan J, Kuang W, Jin Z, Jin F, Xu L, Yu Q, Kong L, Zeng G, Yuan X, Duan Y** 2009 Inhibition of NFκB by activated c-Jun NH2 terminal kinase 1 acts as a switch for C2C12 cell death under excessive stretch. Apoptosis 14:764–770
18. **Schenk S, Horowitz JF** 2007 Acute exercise increases triglyceride synthesis in skeletal muscle and prevents fatty acid-induced insulin resistance. J Clin Invest 117:1690–1698
19. **Nakamura S, Takamura T, Matsuzawa-Nagata N, Takayama H, Misu H, Noda H, Nabemoto S, Kurita S, Ota T, Ando H, Miyamoto K, Kaneko S** 2009 Palmitate induces insulin resistance in H4IIEC3 hepatocytes through reactive oxygen species produced by mitochondria. J Biol Chem 284:14809–14818
20. **Pimenta AS, Gaidhu MP, Habib S, So M, Fediuc S, Mirpourian M, Musheev M, Curi R, Ceddia RB** 2008 Prolonged exposure to palmitate impairs fatty acid oxidation despite activation of AMP-activated protein kinase in skeletal muscle cells. J Cell Physiol 217:478–485
21. **Pu J, Peng G, Li L, Na H, Liu Y, Liu P** 2011 Palmitic acid acutely stimulates glucose uptake via activation of Akt and ERK1/2 in skeletal muscle cells. J Lipid Res 52:1319–1327
22. **Hughes KJ, Meares GP, Chambers KT, Corbett JA** 2009 Repair of nitric oxide-damaged DNA in β-cells requires JNK-dependent GADD45α expression. J Biol Chem 284:27402–27408
23. **Bonnard C, Durand A, Peyrol S, Chanseaume E, Chauvin MA, Morio B, Vidal H, Rieusset J** 2008 Mitochondrial dysfunction results from oxidative stress in the skeletal muscle of diet-induced insulin-resistant mice. J Clin Invest 118:789–800
24. **Anderson EJ, Lustig ME, Boyle KE, Woodlief TL, Kane DA, Lin CT, Price 3rd JW, Kang L, Rabinovitch PS, Szeto HH, Houmard JA, Cortright RN, Wasserman DH, Neufer PD** 2009 Mitochondrial H2O2 emission and cellular redox state link excess fat intake to insulin resistance in both rodents and humans. J Clin Invest 119:573–581
25. **Lee HY, Choi CS, Birkenfeld AL, Alves TC, Jornayvaz FR, Jurczak MJ, Zhang D, Woo DK, Shadel GS, Ladiges W, Rabinovitch PS, Santos JH, Petersen KF, Samuel VT, Shulman GI** 2010 Targeted expression of catalase to mitochondria prevents age-associated reductions in mitochondrial function and insulin resistance. Cell Metab 12:668–674
26. **Hoehn KL, Salmon AB, Hohnen-Behrens C, Turner N, Hoy AJ, Maghzal GJ, Stocker R, Van Remmen H, Kraegen EW, Cooney GJ, Richardson AR, James DE** 2009 Insulin resistance is a cellular antioxidant defense mechanism. Proc Natl Acad Sci USA 106:17787–17792
27. **Houstis N, Rosen ED, Lander ES** 2006 Reactive oxygen species have a causal role in multiple forms of insulin resistance. Nature 440:944–948
28. **Lambertucci RH, Hirabara SM, Silveira Ldos R, Levada-Pires AC, Curi R, Pithon-Curi TC** 2008 Palmitate increases superoxide production through mitochondrial electron transport chain and NADPH oxidase activity in skeletal muscle cells. J Cell Physiol 216:796–804
29. **Gerbitz KD, Gempel K, Brdiczka D** 1996 Mitochondria and diabetes. Genetic, biochemical, and clinical implications of the cellular energy circuit. Diabetes 45:113–126
30. **Adler V, Yin Z, Tew KD, Ronai Z** 1999 Role of redox potential and reactive oxygen species in stress signaling. Oncogene 18:6104–6111
31. **Vinayagamoorthi R, Bobby Z, Sridhar MG** 2008 Antioxidants preserve redox balance and inhibit c-Jun-N-terminal kinase pathway while improving insulin signaling in fat-fed rats: evidence for the role of oxidative stress on IRS-1 serine phosphorylation and insulin resistance. J Endocrinol 197:287–296
32. **Gupte AA, Bomhoff GL, Morris JK, Gorres BK, Geiger PC** 2009 Lipoic acid increases heat shock protein expression and inhibits stress kinase activation to improve insulin signaling in skeletal muscle from high-fat-fed rats. J Appl Physiol 106:1425–1434
33. **Zhang X, Xu A, Chung SK, Cresser JH, Sweeney G, Wong RL, Lin A, Lam KS** 2011 Selective inactivation of c-Jun NH2-terminal kinase in adipose tissue protects against diet-induced obesity and improves insulin sensitivity in both liver and skeletal muscle in mice. Diabetes 60:486–495